NeuroImage: Clinical 28 (2020) 102516

Contents lists available at ScienceDirect

NeuroImage: Clinical

journal homepage: www.elsevier.com/locate/ynicl

Fiber-specific white matter reductions in amyotrophic lateral sclerosis

Luqi Cheng [a], Xie Tang [a], Chunxia Luo [b], Daihong Liu [c], Yuanchao Zhang [a,*], Jiuquan Zhang [c,*]

[a] Key Laboratory for NeuroInformation of Ministry of Education, School of Life Science and Technology, University of Electronic Science and Technology of China, Chengdu 610054, PR China
[b] Department of Neurology, The First Affiliated Hospital, Third Military Medical University, Chongqing 400308, PR China
[c] Department of Radiology, Chongqing University Cancer Hospital, School of Medicine, Chongqing University, Chongqing 400030, PR China

ARTICLE INFO

Keywords:
Amyotrophic lateral sclerosis
Fixel-based analysis
Corticospinal tract
Fiber density
Fiber-bundle cross-section

ABSTRACT

Amyotrophic lateral sclerosis (ALS) is a progressive neurodegenerative disorder characterized by the loss of both upper and lower motor neurons. Studies using metrics derived from the diffusion tensor model have documented decreased fractional anisotropy (FA) and increased mean diffusivity in the corticospinal tract (CST) and the corpus callosum (CC) in ALS. These studies, however, only focused on microstructural white matter (WM) changes, while the macrostructural alterations of WM tracts in ALS remain unknown. Moreover, studies conducted based on the diffusion tensor model cannot provide information related to specific fiber bundles and fail to clarify which biological characteristics are changing. Using a novel fixel-based analytical method that can characterize the fiber density (FD) and the fiber-bundle cross-section (FC), this study investigated both microstructural and macrostructural changes in the WM in a large cohort of patients with ALS (N = 60) compared with demographically matched healthy controls (N = 60). Compared with healthy controls, we found decreased FD, FC and fiber density and cross-section (FDC, a combined measure of the FD and FC) values in the bilateral CST and the middle posterior body of the CC in patients with ALS, suggesting not only microstructural but also macrostructural abnormalities in these fiber bundles. Additionally, we found that the mean FD and FDC values in the bilateral CST were positively correlated with the revised ALS Functional Rating Scale, indicating that these two indices may serve as potential markers for assessing the clinical severity of ALS. Thus, these findings provide initial evidence for the existence of microstructural and macrostructural abnormalities of the fiber bundles in ALS.

1. Introduction

Amyotrophic lateral sclerosis (ALS) is a progressive neurodegenerative disease of the human motor system characterized by loss of both upper motor neurons of the corticospinal tract (CST) and lower motor neurons of the brainstem and spinal cord anterior horns (Turner and Verstraete, 2015). Previous diffusion tensor imaging (DTI) studies using metrics derived from the diffusion tensor model have found focal white matter (WM) abnormalities in ALS, such as decreased fractional anisotropy (FA) and increased mean diffusivity in the CST and the corpus callosum (CC) (Foerster et al., 2013; Turner and Verstraete, 2015). These studies, however, only focused on the microstructural WM changes; thus, the macrostructural alterations of WM tracts in ALS remain unknown. Moreover, DTI studies were limited by the fact that the diffusion tensor model fails to model complex and crossing-fiber populations, which are estimated to exist in up to 90% of the WM voxels in the brain (Jeurissen et al., 2013). In addition, the interpretation of these DTI findings can be difficult since DTI-derived metrics are inherently not fiber-specific (Raffelt et al., 2017) and are sensitive to various microstructural characteristics (Beaulieu, 2002).

Fixel-based analysis (FBA; Raffelt et al., 2017), a recently developed technique for fiber tract-specific statistical analysis, utilizes constrained spherical deconvolution (CSD) to estimate the fiber orientation distributions (FODs) and is thought to be able to resolve multiple fiber populations within a voxel (or fixels) (Raffelt et al., 2015). Using FBA, three quantitative metrics can be obtained, namely, fiber density (FD), fiber-bundle cross-section (FC), and a combined measure of the fiber density and cross-section (FDC). These metrics measure the microscopic changes in the density of fiber bundles within a given voxel, the macroscopic changes in cross-sectional area perpendicular to a fiber bundle, and both the microscopic and macroscopic effects described above. In previous neuroimaging studies, FBA has been successfully used

* Corresponding authors.
E-mail addresses: yuanchao.zhang8@gmail.com (Y. Zhang), zhangjq_radiol@foxmail.com (J. Zhang).

https://doi.org/10.1016/j.nicl.2020.102516
Received 21 October 2020; Received in revised form 23 November 2020; Accepted 25 November 2020
Available online 2 December 2020

to characterize WM abnormalities in various diseased populations, such as Alzheimer's disease (Mito et al., 2018), multiple sclerosis (Gajamange et al., 2018) and autism spectrum disorder (Dimond et al., 2019). Reportedly, FBA-based metrics have greater structural specificity and are more easily interpretable than traditional DTI-derived metrics (Raffelt et al., 2017). Hence, simultaneous investigations of the WM microstructural and macrostructural alterations in ALS using FBA may provide new insight into the pathophysiology of ALS.

In this study, we aimed to utilize FBA to explore the mechanisms underlying the WM degeneration in a large cohort of patients with ALS (N = 60) compared with demographically matched healthy controls (N = 60). Based on the existing literature (Smith, 1960; Turner and Verstraete, 2015), we hypothesized that compared with healthy controls, patients with ALS would exhibit not only microstructural alterations (e.g., decreased FD) but also macrostructural alterations (e.g., decreased FC) in tracts associated with motor functions, such as the CST and CC.

2. Material and methods

2.1. Participants

A total of 120 right-handed subjects, including 60 patients with ALS (39 males, mean age 48.77 years old, range 26–69) and 60 healthy controls (39 males, mean age 48.15 years old, range 24–70), were included in this study. These subjects had also participated in our previous neuroimaging study (Qiu et al., 2019). Briefly, all patients with ALS met the El Escorial criteria for probable or definite ALS (Brooks et al., 2000) and were recruited. The clinical status of all patients was assessed with the revised ALS Functional Rating Scale (ALSFRS-R) (Cedarbaum et al., 1999). Disease duration was calculated from symptom onset to the scanning date (months), and the rate of disease progression was estimated by the following metric: (48-ALSFRS-R score)/(disease duration). The exclusion criteria were as follows: (i) a family history of motor neuron diseases; (ii) a clinical diagnosis of frontotemporal dementia (Brooks et al., 2000); (iii) cognitive impairment (Montreal Cognitive Assessment score < 26) (Nasreddine et al., 2005); and (iv) other major systemic, psychiatric, and neurological illnesses. The sex- and age-matched healthy controls were free of a previous history of neurological or psychiatric diseases and were recruited from the local community. The detailed demographic and relevant clinical data of all subjects are shown in Table 1. Ethics approval for all procedures was obtained from the Medical Research Ethics Committee of Southwest Hospital. All subjects gave their written informed consent according to the Helsinki Declaration.

Table 1
Demographic and clinical characteristics of the subjects.

	ALS (N = 60)	HC (N = 60)	*p* value
Mean age in years (range)	48.77(26–69)	48.15 (24–70)	0.73
Sex (male/female)	39/21	39/21	1.00
Mean disease duration in months (range)	21.05(2–132)	–	–
Mean disease progression rate (range)	1.36 (0.02–6.50)	–	–
Mean ALSFRS-R (range)	32.62(16–45)	–	–
MoCA score (range)	27.38(26–30)	27.63 (26–30)	0.29
Limb/bulbar/both onset	47/12/1	–	–
Classic/UMN-D/LMN-D/PMA/PLS	43/7/7/2/1	–	–

ALSFRS-R, Revised Amyotrophic Lateral Sclerosis Functional Rating Scale; MoCA, Montreal Cognitive Assessment. HC: healthy controls
The ALS patients were subdivided into 5 phenotypes: classic, upper motor neuron dominant (UMN-D), lower motor neuron dominant (LMN-D), progressive muscular atrophy (PMA) and primary lateral sclerosis (PLS).

2.2. MRI acquisition

Image acquisition was performed using a Siemens 3 T Tim Trio scanner with an eight-channel head coil. Diffusion-weighted imaging data were acquired using a single-shot twice-refocused spin echo sequence for each subject. The following parameters were used: 64 diffusion-weighted (b = 1000 s/mm^2) images and a nondiffusion-weighted (b = 0 s/mm^2) image; TR/TE = 10,000/92 ms; matrix = 128 × 124; field of view (FOV) = 256 × 248 mm^2; thickness = 2 mm; 75 axial slices with no slice gap. T1-weighted images were collected for each subject using a three-dimensional magnetization-prepared rapid gradient-echo imaging sequence with 176 contiguous 1-mm sagittal slices (TR/TE = 1900/2.52 ms; inversion time = 900 ms; flip angle = 9°; matrix = 256 × 256; thickness = 1.0 mm, voxel size = 1 × 1 × 1 mm^3, and no slice gap).

2.3. Image processing

All preprocessing steps of diffusion-weighted images were performed using the MRtrix3 package (Tournier et al., 2019). Principal preprocessing of diffusion-weighted images included denoising (Veraart et al., 2016), eddy-current and motion correction (Andersson and Sotiropoulos, 2016), bias field correction (Tustison et al., 2010), and spatial upsampling by a factor of two using cubic b-spline interpolation (Raffelt et al., 2012a). Intensity normalization was performed across all subjects using the median intensity of the b = 0 s/mm^2 image within a WM mask.

Following the preprocessing steps, FODs were computed using single-shell 3-tissue CSD (SS3T-CSD) for each subject using group averaged response functions for WM, gray matter, and cerebrospinal fluid (Dhollander and Connelly, 2016; Dhollander et al., 2017). Then, a study-specific population FOD template was generated by an iterative linear and nonlinear registration and averaging approach (Raffelt et al., 2011) using FOD images from 40 subjects (20 ALS patients and 20 healthy controls). Finally, each subject's FOD image was nonlinearly registered to the population FOD template (Raffelt et al., 2011, 2012b).

Whole-brain probabilistic tractography was performed on the population FOD template. Twenty million streamlines were generated first. To reduce reconstruction biases, the spherical-deconvolution informed filtering of tractograms (SIFT) algorithm was then applied to filter it down to two million streamlines (Smith et al., 2013).

The fixel-based metrics of FD, FC and the combined measure of FDC were derived for each subject across all WM fixels. Details of the FBA method and interpretations for these metrics have been described by Raffelt *et al.* (Raffelt et al., 2017) (Fig. 1A). In brief, FD is calculated as the integral of the FOD along a particular direction and is proportional to the volume of the intra-axonal compartment of fibers oriented in that direction (Raffelt et al., 2012a). FD is sensitive to alterations at the microstructural level within a voxel. By warping a subject's FOD image into template space, the FC is calculated from the warp field perpendicular to the fixel orientation (Raffelt et al., 2017). The FC is a relative measure and sensitive to macrostructural and morphological changes of a fiber bundle cross-section. FDC is a combined metric multiplying FD and the FC at each fixel, which reflects both microscopic axonal changes and macroscopic changes within a fiber bundle.

In this study, a whole-brain FBA was first performed to identify regions associated with altered FD, FC, and FDC in patients with ALS. Subsequently, we further conducted tract-of-interest FBA to investigate potential degeneration of selective fiber bundles in patients with ALS. Firstly, based on the results of whole-brain FBA, the fixels that exhibited significant decreases in the FDC metric in patients with ALS were categorized into 3 WM tracts, using the JHU DTI-based WM atlases (Mori et al., 2005; Wakana et al., 2007). Secondly, for each tract, streamlines, which were selected from the template tractogram using an approach with two regions of interest, were used to create a fixel-mask. These fixel-masks overlapped with the fixels that exhibited significant

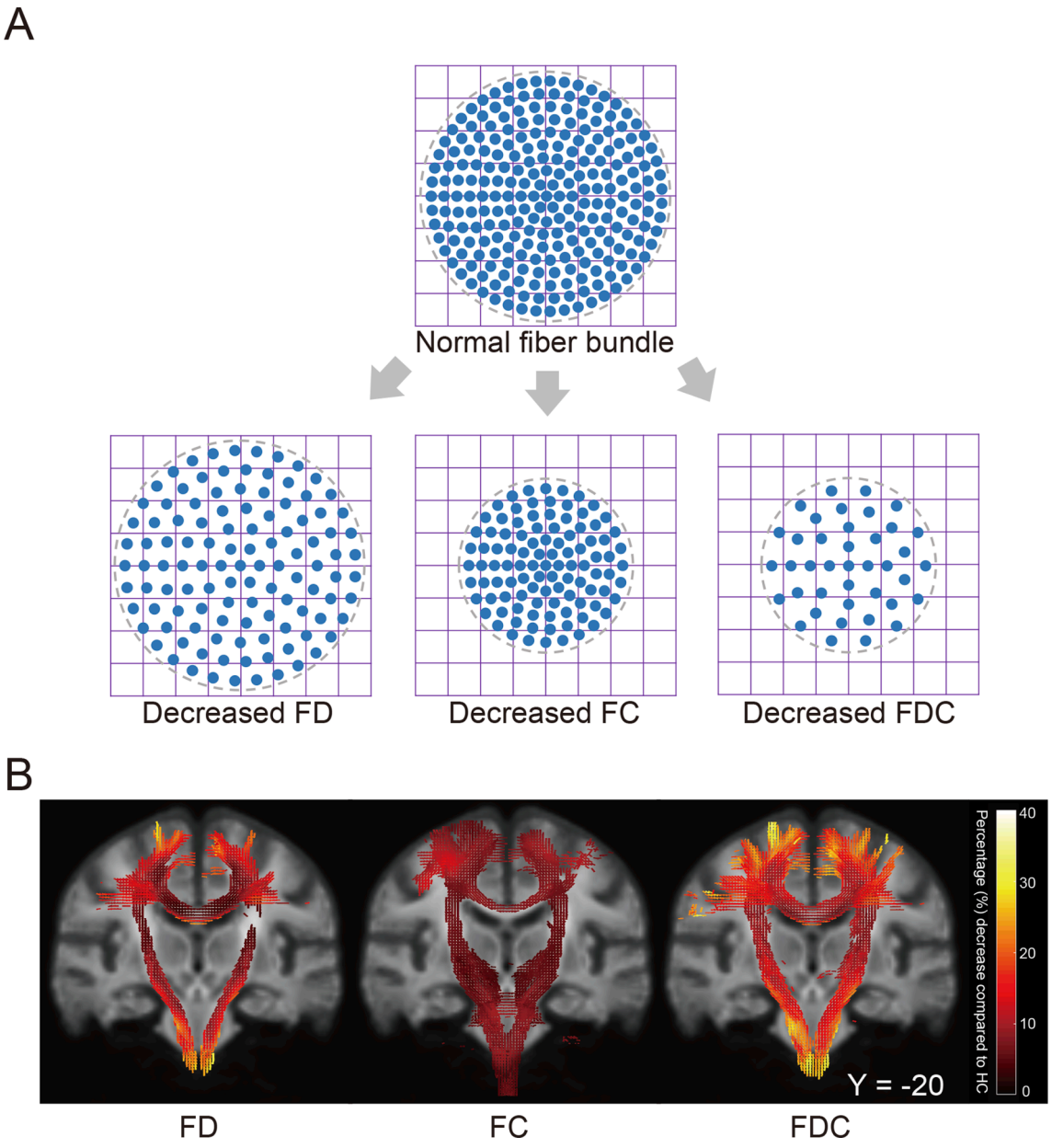

Fig. 1. (A) A schematic showing a fiber bundle cross-section with changes of fiber density (FD), fiber bundle cross-section (FC) and fiber density and cross-section (FDC, a product of the FD and FC) values. Each blue circle represents the cross-section of an axon, the large gray circle represents the cross-section of a fiber bundle, and the grid represents imaging voxels. (B) Fiber-specific reductions in patients with ALS compared with healthy controls (HC). Streamline segments including streamlines that correspond to significant fixels (FWE-corrected p-value < 0.05) were cropped from the template tractogram. Streamlines were colored by percentage effect decrease in patients with ALS compared with HC for FD, FC and FDC. Significant streamlines were rendered on the population template. CST, the corticospinal tract; CC, the corpus callosum. (For interpretation of the references to colour in this figure legend, the reader is referred to the web version of this article.)

decreases in the FDC metric. Finally, the mean FD, FC and FDC within these fixel-masks were calculated for each subject.

2.4. Tract-of-interest WM volumetric analysis

The WM volume map was obtained from the T1-weighted images of each subject to examine the WM macrostructural changes in patients with ALS. Preprocessing of T1-weighted images was performed using the Computational Analysis Tool 12 (CAT12; http://www.neuro.uni-jena.de/cat/) implemented in Statistical Parametric Mapping 12 (SPM12; http://www.fil.ion.ucl.ac.uk/spm) software. Principal preprocessing steps included spatial normalization, segmentation into grey matter, WM, and cerebrospinal fluid tissue classes with default settings in 1.5 mm isotropic MNI space, modulation, and smoothing with an 8-mm FWHM Gaussian kernel. Subsequently, the mean WM volume of each tract defined in the tract-of-interest FBA was extracted for each subject by first transforming the tracts into MNI space and then averaging the WM volumes across the voxels of the corresponding tract.

2.5. Statistical analysis

For the whole-brain FBA, between-group contrasts of FD, FC, and FDC were performed for each WM fixel by fitting a general linear model (GLM) with age and sex as nuisance covariates. Familywise error (FWE)-corrected p-values were then assigned to each fixel using nonparametric permutation testing with 5000 permutations. The significance level was set at FWE corrected $p < 0.05$.

For the tract-of-interest FBA and WM volumetric analysis, the GLM

used in the whole-brain FBA was repeated to test for the between-group difference in the FD, FC, FDC, and WM volume. Bonferroni correction was then used for multiple comparisons for all tracts, with statistical significance set at $p < 0.05$. In the patient group, correlation analysis was performed to examine the relationship between the mean values of these metrics of the tracts and the ALSFRS-R scores. In addition, correlation analysis was also performed to explore the relationship between FBA metrics (i.e., FD, FC and FDC) and WM volume for each group.

2.6. Post-hoc discriminant analysis

We further investigated the sensitivity, specificity and accuracy to distinguish patients with ALS from healthy controls, using a model including the FBA metrics (i.e., FD, FC and FDC) with significant between-group differences in the tract-of-interest FBA, according to the previous study (Trojsi et al., 2017). This discriminant analysis was performed using a stepwise method (Wilks' lambda) in SPSS (version 25).

3. Results

3.1. Whole-brain FBA

Compared with healthy controls, the whole-brain FBA found significantly decreased FD, FC, and FDC values in patients with ALS (FWE-corrected p-value < 0.05), involving the bilateral CST and the middle posterior body of the CC (Fig. 1B). In the figure, streamlines are colored by the magnitude of decreases in patients with ALS compared to control subjects. These fiber bundles were used for the subsequent tract-of-interest FBA.

3.2. Tract-of-interest FBA

Tracts including the bilateral CST and the middle posterior body of the CC identified in whole-brain FBA were extracted and demonstrated (Fig. 2A). Further tractwise between-group comparisons showed significantly decreased FD, FC and FDC in the bilateral CST and the middle posterior body of the CC (Bonferroni corrected p-value < 0.05) in patients with ALS compared with healthy controls (Fig. 2B).

In the patient group, the mean FD and FDC values of the bilateral CST were found to be positively correlated with the ALSFRS-R scores (Fig. 3). No significant correlations were found between the mean FC values and the ALSFRS-R scores.

3.3. Tract-of-interest WM volumetric analysis

Compared with healthy controls, patients with ALS showed a significant decrease in WM volume in the bilateral CST (Bonferroni corrected p-value < 0.05) and a trend towards decreased WM volume in the middle posterior body of the CC (uncorrected $p = 0.028$) (Fig. 4A). For each group, the WM volume of these tracts was strongly correlated with the FC and FDC, and was not or only mildly correlated with the FD (Fig. 4B).

3.4. Post-hoc discriminant analysis

Discriminant analysis showed that, overall, the combination of all FBA metrics in the bilateral CST exhibited the best sensitivity, specificity and accuracy in distinguishing ALS patients from healthy controls, and that the FD and FDC in all tracts exhibited higher sensitivity, specificity and accuracy than the FC (Table 2).

4. Discussion

In the present study, we applied a recently developed FBA framework to examine fiber tract-specific WM degeneration in patients with ALS. Compared with healthy controls, patients with ALS showed decreased FD values (assessing WM microstructural changes), as well as decreased FC (assessing WM macrostructural changes) and decreased FDC (assessing both microstructural and macrostructural changes) values in the bilateral CST and the middle posterior body of the CC. In addition, WM volume of these tracts was found to be decreased in patients with ALS and strongly correlated with the FC and FDC. In the patient group, the mean FD and FDC values of the bilateral CST were positively correlated with the ALSFRS-R scores. Our findings provide initial evidence for the existence of both microstructural and macrostructural abnormalities of the fiber bundles in ALS.

Our findings of decreased FD, FC and FDC values in the bilateral CST are of particular interest in ALS. Indeed, the CST is a motor fiber pathway that originates in the primary motor cortex and contains fibers from the upper motor neurons that synapse on the lower motor neurons (Seo and Jang, 2013). The CST is essential for the motor system as it plays crucial roles in mediating voluntary distal movements (Welniarz et al., 2017). As such, one may speculate that the observed decreases in FD, FC and FDC values in the CST contributed to the clinical signs of patients with ALS, such as foot drop, difficulty walking, and loss of fine motor skills (Gordon, 2013). In addition, we also showed decreased FD, FC and FDC values in the middle posterior body of the CC in patients with ALS compared with healthy controls. The CC is the largest fiber bundle of the brain interconnecting the two hemispheres and plays an important role in interhemispheric communication (van der Knaap and van der Ham, 2011; Zhang et al., 2017). More specifically, the middle posterior body of the CC interconnects the primary motor cortices of the two hemispheres and has been implicated in bimanual coordination (Wahl et al., 2007). Hence, the alteration in the middle posterior body of the CC may reflect abnormal interhemispheric information transfer between the bilateral primary motor cortices and underlie the mirror movements in ALS (Wittstock et al., 2011), consistent with our previous report of disrupted interhemispheric functional and structural connectivity in patients with ALS (Zhang et al., 2017).

Our findings of significant microstructural abnormalities in the bilateral CST and the middle posterior body of the CC in ALS revealed by decreased FD are consistent with previous reports using DTI and high-angular resolution diffusion imaging (HARDI) (Kalra et al., 2020; Kassubek et al., 2018; Müller et al., 2020, 2016; Qiu et al., 2019; Trojsi et al., 2017, 2013). Specifically, some HARDI studies showed a highly significant decrease of generalized FA and fiber length and density in the CST and CC (Trojsi et al., 2017, 2013). Based on large-scale multicenter DTI data, more recent prospective studies demonstrated the most significant FA alterations in the CST using whole-brain-based spatial statistics (Kalra et al., 2020; Kassubek et al., 2018; Müller et al., 2020, 2016). Of note, however, these studies also found varying degrees of extra-motor involvement in patients with ALS, which was not found in the present study. The exact mechanisms underlying such inconsistency remain unclear and might relate to factors such as differences in the demographic characteristics of the patients with ALS (i.e., with or without significant cognitive impairment, pathological stages, disease duration, *etc*), and/or the sensitivity of different analytical methods, and so on. As FA is not fiber-specific and is easily affected by crossing-fiber populations, FA changes in voxels containing more than one fiber bundle may be attributed to the fiber bundles that lack actual damage (Raffelt et al., 2012a, 2017). In contrast, FBA is fiber-specific; therefore, one is able to discriminate which fiber bundles were affected using this approach (Raffelt et al., 2017). Moreover, unlike FA, which is unable to clarify which biological characteristics are changing, FD values are more biologically meaningful since this metric measures the microstructural changes in the density of a fiber bundle within a voxel. Hence, our result of decreased FD provided new evidence for the microstructural abnormalities in these fiber bundles by showing decreased intra-axonal volume in ALS. More interestingly, the present study also found significant macrostructural abnormalities in patients with ALS, as indicated by decreased FC in the bilateral CST and the middle posterior body of the

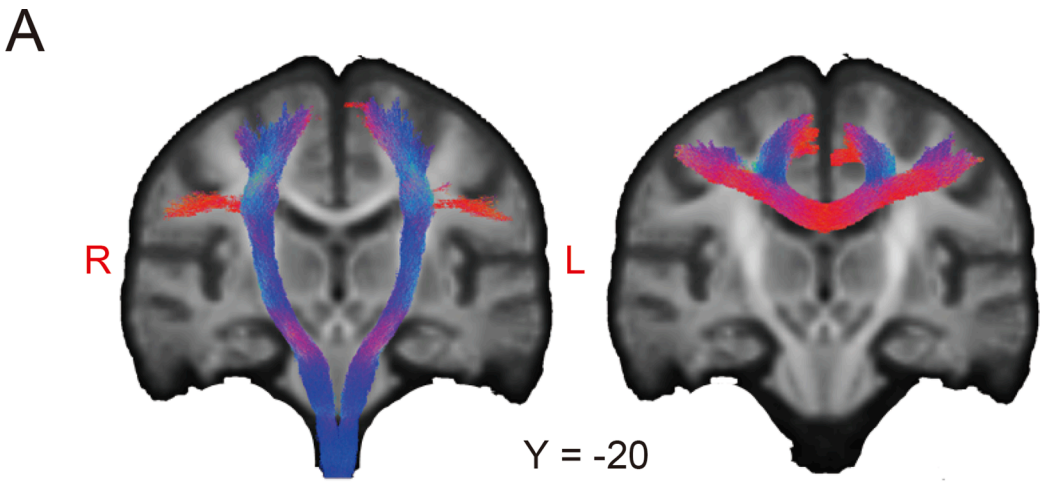

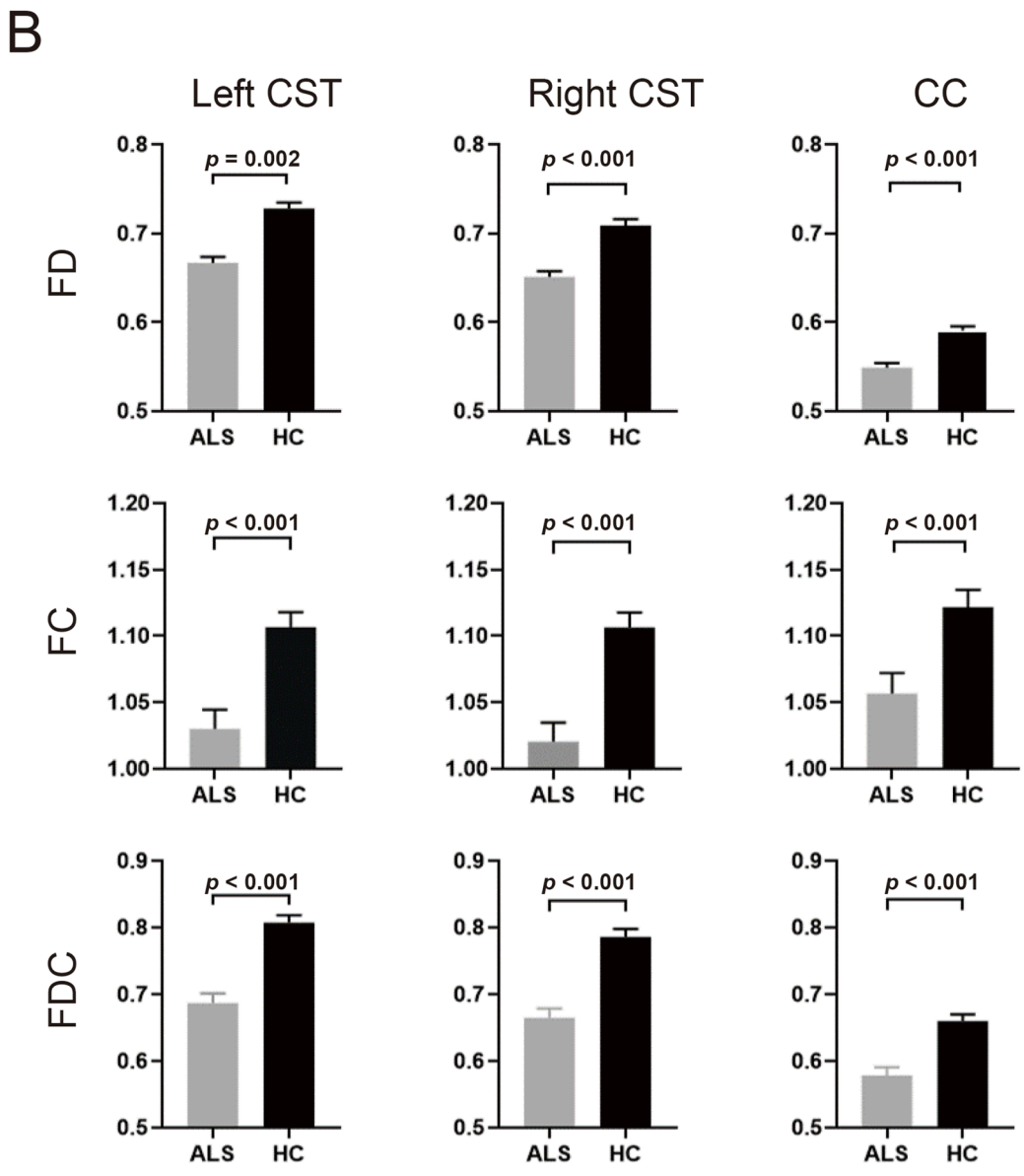

Fig. 2. White matter abnormalities from tract-of-interest fixel-based analysis (FBA) in patients with ALS compared with healthy controls. (A) Tracts including the bilateral corticospinal tracts (CST) and the corpus callosum (CC) identified in whole-brain FBA were rendered on the population template. (B) Mean fiber density (FD), fiber-bundle cross-section (FC), and fiber density and cross-section (FDC) values of the CC and the bilateral CST in patients with ALS and healthy controls (HC). The error bar indicates the standard error of the mean.

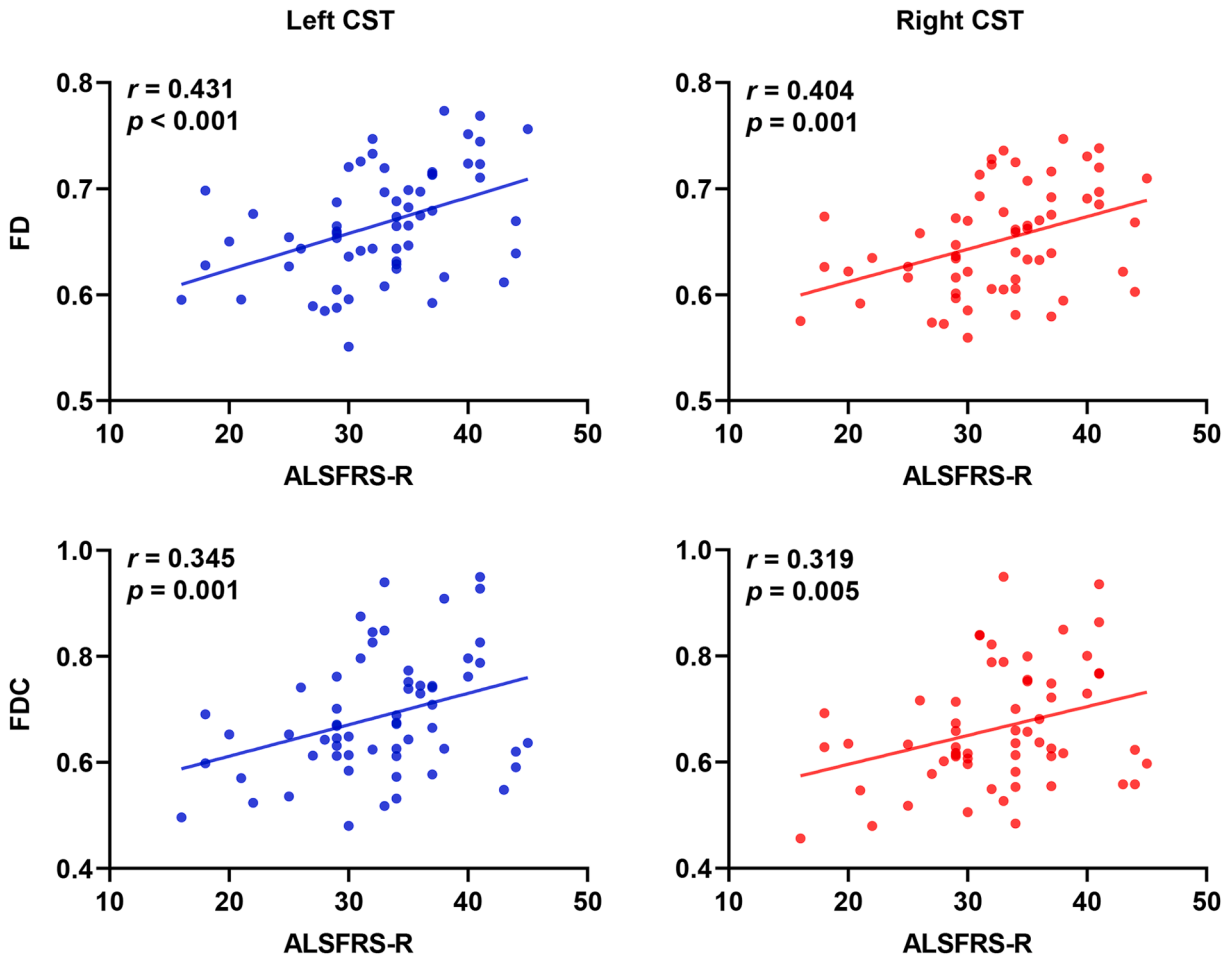

Fig. 3. Positive correlation between the mean fiber density (FD) and fiber density and cross-section (FDC) of the bilateral corticospinal tracts (CST) and ALSFRS-R scores in patients with ALS. ALSFRS-R, ALS Functional Rating Scale.

CC. This finding is consistent with a previous texture-based study (Ishaque et al., 2019) reporting texture alterations in the CST of patients with ALS, and is supported by our result of significant WM volume reductions in the CST of patients with ALS, and strong positive correlations between FC and WM volume of CST in both groups. As FC measures the macrostructural changes in the cross-sectional area perpendicular to the fiber orientation rather than along the length of a fiber bundle, changes in FC can better reflect differences in the number of axons ('the ability to relay information') (Raffelt et al., 2017). Therefore, the decreased FC in the CST and CC in ALS may suggest an inability to relay information between the upper and lower motor neurons, as well as between the primary motor cortices of the bilateral hemispheres. In addition, this study found decreased FDC (a product of the FD and FC) in the CST and the middle posterior body of the CC in patients with ALS. These findings, together with the result of concurrent decrease in FD and FC, further confirmed the existence of both microstructural and macrostructural abnormalities in ALS. Indeed, previous pathological studies have demonstrated a significant reduction in motor axon density in ALS (Brownell et al., 1970; Smith, 1960), which may manifest as decreased FD in the CST and CC. As axonal loss continues, extracellular spaces may be increased due to myelin and axon debris resulting from inflammatory infiltrates or gliosis (Hughes, 1982; Turner et al., 2012). After debris removal, the fiber bundles become atrophic, which may manifest as decreased FC in the CST and CC. As such, a combination of these two biological processes may have contributed to the decreased FDC values in ALS.

In the patient group, we found a positive correlation between the mean FD of the bilateral CST and the ALSFRS-R scores, which is in agreement with previous findings (Kalra et al., 2020; Trojsi et al., 2017). These results indicate that WM microstructural abnormalities might be the anatomical substrates underlying motor symptoms in ALS. As such, the FD of the bilateral CST may serve as a potential marker for assessing the clinical severity of patients with ALS. Of note, the mean FDC, rather than the FC, of the bilateral CST was found to be positively correlated with the ALSFRS-R scores of the patient group, indicating that the correlation between the FDC and the ALSFRS-R scores may be mainly driven by the relationship between the FD and the ALSFRS-R scores. These correlational results may illustrate a temporal sequence of the WM microstructural and macrostructural abnormalities in ALS; that is, the WM macrostructural abnormalities emerge along with the continuation of the WM microstructural abnormalities.

Despite the technical advantages of FBA, there are some limitations that should be addressed regarding this study. First, the present study was limited by a cross-sectional design, which did not allow us to characterize the progression of the WM damage in ALS. Longitudinal follow-up research may be conducive to uncovering the dynamic pattern of these brain abnormalities with the development of the disease. Second, clinical signs of upper motor neuron impairment were not evaluated. Future studies with more detailed clinical assessments are needed to investigate the relationship between clinical assessments and FBA metrics. Third, the diffusion data of this study were acquired using sufficient angular resolution to provide a valid and robust analysis, yet the acquisition of the relatively low b-values is not optimal for the CSD model. To counteract this limitation, we used the state-of-the-art SS3T-CSD method (Dhollander and Connelly, 2016) that considers the presence of the three tissue types and may provide additional information

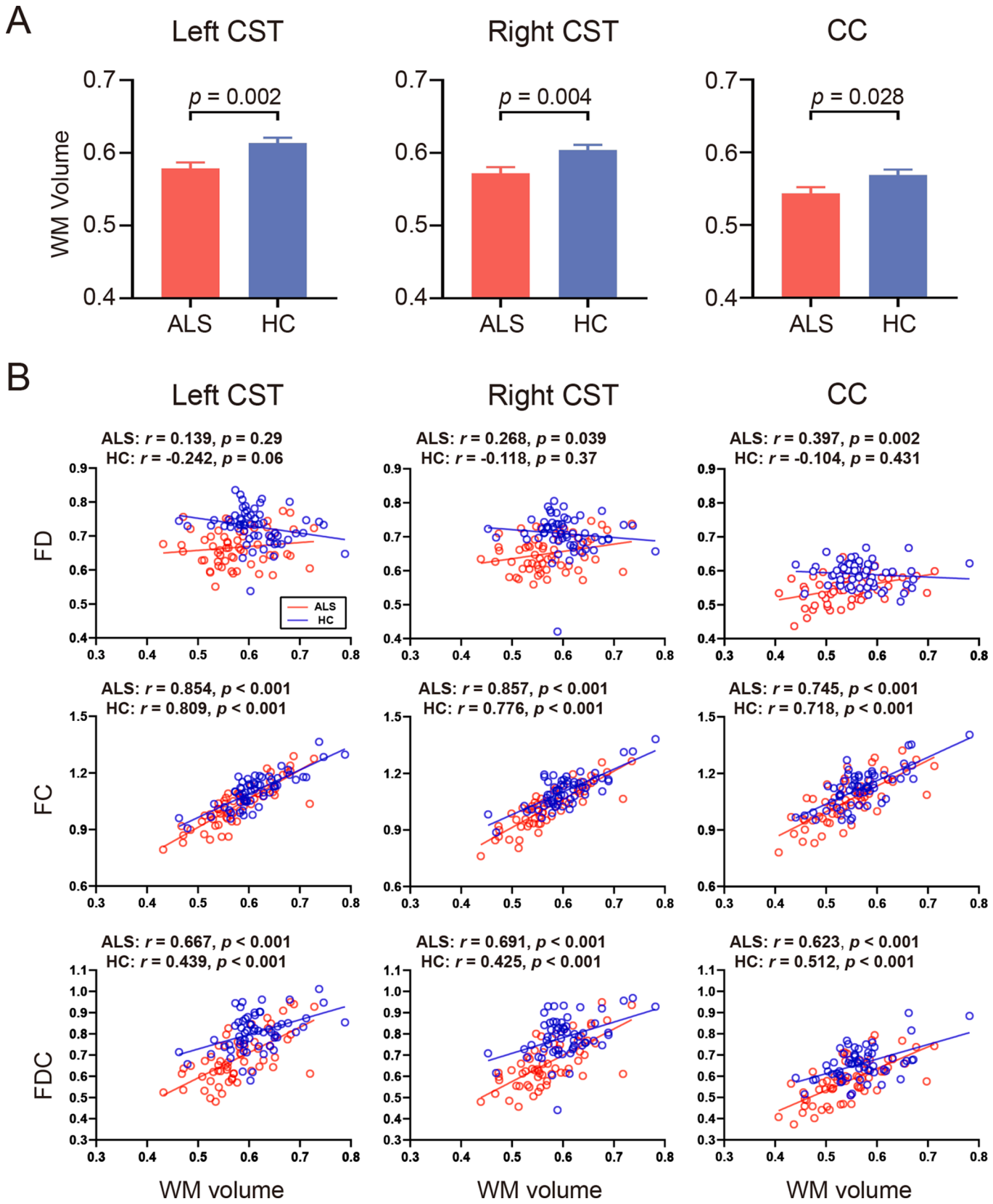

Fig. 4. Tract-of-interest white matter (WM) volumetric analysis. (A) Mean WM volume of the bilateral corticospinal tracts (CST) and the corpus callosum (CC) in patients with ALS and healthy controls (HC). The error bar indicates the standard error of the mean. (B) Correlation between FBA metrics and WM volume for the tracts in each group. FD, fiber density; FC, fiber-bundle cross-section; FDC, fiber density and cross-section.

Table 2
The post hoc discriminant analysis between patients with ALS and healthy controls.

	FD	FC	FDC	FD + FC + FDC Enter method	FD + FC + FDC Stepwise method
Left corticospinal tract					
Wilks' Lambda	0.737	0.874	0.739	0.701	0.703
Sensitivity	68.3%	63.3%	73.3%	73.3%	73.3%
Specificity	76.7%	68.3%	75%	83.3%	80%
Accuracy	72.5%	65.8%	74.2%	78.3%	76.7%
Right corticospinal tract					
Wilks' Lambda	0.765	0.839	0.746	0.717	0.746
Sensitivity	71.7%	68.3%	71.7%	70%	71.7%
Specificity	80%	68.3%	76.7%	86.7%	76.7%
Accuracy	75.8%	68.3%	74.2%	78.3%	74.2%
Corpus callosum					
Wilks' Lambda	0.774	0.919	0.824	0.749	0.774
Sensitivity	61.7%	63.3%	66.7%	61.7%	61.7%
Specificity	68.3%	66.7%	70%	75%	68.3%
Accuracy	65%	65%	68.3%	68.3%	65%

FD, fiber density; FC, fiber bundle cross-section; FDC, fiber density and cross-section.

that can be used in microstructural mathematical models (Dhollander et al., 2017). Future studies should use a more suitable acquisition with higher b-values, higher angular resolution and multishells to increase the statistical power and sensitivity.

5. Conclusion

Using a novel FBA method, the present study found significantly decreased FD, FC and FDC in the bilateral CST and the middle posterior body of the CC in patients with ALS, suggesting both microstructural abnormalities and macrostructural abnormalities in these fiber bundles. In addition, we found that the FD and FDC in the bilateral CST were positively correlated with the ALSFRS-R scores in the patient group, suggesting that these two indices of the CST may serve as potential markers for assessing the clinical severity of patients with ALS. Our findings provide initial evidence for the existence of both microstructural and macrostructural abnormalities of the fiber bundles in ALS.

CRediT authorship contribution statement

Luqi Cheng: Conceptualization, Methodology, Validation, Formal analysis, Data curation, Writing - original draft, Writing - review & editing. **Xie Tang:** Investigation, Writing - review & editing. **Chunxia Luo:** Resources, Writing - review & editing. **Daihong Liu:** Resources, Writing - review & editing. **Yuanchao Zhang:** Conceptualization, Methodology, Validation, Formal analysis, Data curation, Resources, Writing - original draft, Writing - review & editing. **Jiuquan Zhang:** Resources, Funding acquisition, Writing - review & editing.

Declaration of Competing Interest

The authors declare that they have no known competing financial interests or personal relationships that could have appeared to influence the work reported in this paper.

Acknowledgments

This study has received funding by the National Natural Science Foundation of China (Grant No. 82071883), the combination projects of medicine and engineering of the Fundamental Research Funds for the Central Universities in 2019 (Project No. 2019CDYGYB008), the Chongqing key medical research project of combination of science and medicine (Grant No. 2019ZDXM007), and the 2019 SKY Imaging Research Fund of the Chinese International Medical Foundation (Project No. Z-2014-07-1912-10).

References

Andersson, J.L., Sotiropoulos, S.N., 2016. An integrated approach to correction for off-resonance effects and subject movement in diffusion MR imaging. NeuroImage 125, 1063–1078.
Beaulieu, C., 2002. The basis of anisotropic water diffusion in the nervous system–a technical review. NMR Biomedicine 15, 435–455.
Brooks, B.R., Miller, R.G., Swash, M., Munsat, T.L., 2000. El Escorial revisited: revised criteria for the diagnosis of amyotrophic lateral sclerosis. Amyotrophic Lateral Sclerosis and Other Motor Neuron Disorders 1, 293–299.
Brownell, B., Oppenheimer, D., Hughes, J.T., 1970. The central nervous system in motor neurone disease. J. Neurol. Neurosurg. Psychiatry 33, 338–357.
Cedarbaum, J.M., Stambler, N., Malta, E., Fuller, C., Hilt, D., Thurmond, B., Nakanishi, A., 1999. The ALSFRS-R: a revised ALS functional rating scale that incorporates assessments of respiratory function. J. Neurol. Sci. 169, 13–21.
Dhollander, T., Connelly, A., 2016. A novel iterative approach to reap the benefits of multi-tissue CSD from just single-shell (+ b= 0) diffusion MRI data. Proc ISMRM, p. 3010.
Dhollander, T., Raffelt, D., Connelly, A., 2017. Towards interpretation of 3-tissue constrained spherical deconvolution results in pathology. Intl. Soc. Mag. Reson. Med. Proc. 1815.
Dimond, D., Schuetze, M., Smith, R.E., Dhollander, T., Cho, I., Vinette, S., Ten Eycke, K., Lebel, C., McCrimmon, A., Dewey, D., 2019. Reduced white matter fiber density in autism spectrum disorder. Cereb. Cortex 29, 1778–1788.
Foerster, B.R., Welsh, R.C., Feldman, E.L., 2013. 25 years of neuroimaging in amyotrophic lateral sclerosis. Nature Reviews Neurology 9, 513–524.
Gajamange, S., Raffelt, D., Dhollander, T., Lui, E., van der Walt, A., Kilpatrick, T., Fielding, J., Connelly, A., Kolbe, S., 2018. Fibre-specific white matter changes in multiple sclerosis patients with optic neuritis. NeuroImage: Clinical 17, 60–68.
Gordon, P.H., 2013. Amyotrophic lateral sclerosis: an update for 2013 clinical features, pathophysiology, management and therapeutic trials. Aging and disease 4, 295.
Hughes, J., 1982. Pathology of amyotrophic lateral sclerosis. Adv. Neurol. 36, 61–74.
Ishaque, A., Mah, D., Seres, P., Luk, C., Johnston, W., Chenji, S., Beaulieu, C., Yang, Y.H., Kalra, S., 2019. Corticospinal tract degeneration in ALS unmasked in T1-weighted images using texture analysis. Hum. Brain Mapp. 40, 1174–1183.
Jeurissen, B., Leemans, A., Tournier, J.D., Jones, D.K., Sijbers, J., 2013. Investigating the prevalence of complex fiber configurations in white matter tissue with diffusion magnetic resonance imaging. Hum. Brain Mapp. 34, 2747–2766.
Kalra, S., Müller, H.-P., Ishaque, A., Zinman, L., Korngut, L., Genge, A., Beaulieu, C., Frayne, R., Graham, S.J., Kassubek, J., 2020. A prospective harmonized multicenter DTI study of cerebral white matter degeneration in ALS. Neurology 95, e943–e952.
Kassubek, J., Müller, H.-P., Del Tredici, K., Lulé, D., Gorges, M., Braak, H., Ludolph, A.C., 2018. Imaging the pathoanatomy of amyotrophic lateral sclerosis in vivo: targeting a propagation-based biological marker. J. Neurol. Neurosurg. Psychiatry 89, 374–381.
Mito, R., Raffelt, D., Dhollander, T., Vaughan, D.N., Tournier, J.-D., Salvado, O., Brodtmann, A., Rowe, C.C., Villemagne, V.L., Connelly, A., 2018. Fibre-specific white matter reductions in Alzheimer's disease and mild cognitive impairment. Brain 141, 888–902.
Mori, S., Wakana, S., Van Zijl, P.C., Nagae-Poetscher, L., 2005. MRI atlas of human white matter. Elsevier.
Müller, H.-P., Del Tredici, K., Lulé, D., Müller, K., Weishaupt, J.H., Ludolph, A.C., Kassubek, J., 2020. In vivo histopathological staging in C9orf72-associated ALS: A tract of interest DTI study. NeuroImage: Clinical 102298.
Müller, H.-P., Turner, M.R., Grosskreutz, J., Abrahams, S., Bede, P., Govind, V., Prudlo, J., Ludolph, A.C., Filippi, M., Kassubek, J., 2016. A large-scale multicentre cerebral diffusion tensor imaging study in amyotrophic lateral sclerosis. J. Neurol. Neurosurg. Psychiatry 87, 570–579.
Nasreddine, Z.S., Phillips, N.A., Bédirian, V., Charbonneau, S., Whitehead, V., Collin, I., Cummings, J.L., Chertkow, H., 2005. The Montreal Cognitive Assessment, MoCA: a brief screening tool for mild cognitive impairment. J. Am. Geriatr. Soc. 53, 695–699.
Qiu, T., Zhang, Y., Tang, X., Liu, X., Wang, Y., Zhou, C., Luo, C., Zhang, J., 2019. Precentral degeneration and cerebellar compensation in amyotrophic lateral sclerosis: A multimodal MRI analysis. Hum. Brain Mapp. 40, 3464–3474.
Raffelt, D., Tournier, J.-D., Fripp, J., Crozier, S., Connelly, A., Salvado, O., 2011. Symmetric diffeomorphic registration of fibre orientation distributions. NeuroImage 56, 1171–1180.
Raffelt, D., Tournier, J.-D., Rose, S., Ridgway, G.R., Henderson, R., Crozier, S., Salvado, O., Connelly, A., 2012a. Apparent fibre density: a novel measure for the analysis of diffusion-weighted magnetic resonance images. NeuroImage 59, 3976–3994.
Raffelt, D., Tournier, J.D., Crozier, S., Connelly, A., Salvado, O., 2012b. Reorientation of fiber orientation distributions using apodized point spread functions. Magn. Reson. Med. 67, 844–855.
Raffelt, D.A., Smith, R.E., Ridgway, G.R., Tournier, J.-D., Vaughan, D.N., Rose, S., Henderson, R., Connelly, A., 2015. Connectivity-based fixel enhancement: Whole-brain statistical analysis of diffusion MRI measures in the presence of crossing fibres. NeuroImage 117, 40–55.

Raffelt, D.A., Tournier, J.-D., Smith, R.E., Vaughan, D.N., Jackson, G., Ridgway, G.R., Connelly, A., 2017. Investigating white matter fibre density and morphology using fixel-based analysis. NeuroImage 144, 58–73.
Seo, J., Jang, S., 2013. Different characteristics of the corticospinal tract according to the cerebral origin: DTI study. Am. J. Neuroradiol. 34, 1359–1363.
Smith, M.C., 1960. Nerve fibre degeneration in the brain in amyotrophic lateral sclerosis. J. Neurol. Neurosurg. Psychiatry 23, 269.
Smith, R.E., Tournier, J.-D., Calamante, F., Connelly, A., 2013. SIFT: Spherical-deconvolution informed filtering of tractograms. NeuroImage 67, 298–312.
Tournier, J.-D., Smith, R., Raffelt, D., Tabbara, R., Dhollander, T., Pietsch, M., Christiaens, D., Jeurissen, B., Yeh, C.-H., Connelly, A., 2019. MRtrix3: A fast, flexible and open software framework for medical image processing and visualisation. NeuroImage, 116137.
Trojsi, F., Caiazzo, G., Di Nardo, F., Fratello, M., Santangelo, G., Siciliano, M., Femiano, C., Russo, A., Monsurrò, M.R., Cirillo, M., 2017. High angular resolution diffusion imaging abnormalities in the early stages of amyotrophic lateral sclerosis. J. Neurol. Sci. 380, 215–222.
Trojsi, F., Corbo, D., Caiazzo, G., Piccirillo, G., Monsurrò, M.R., Cirillo, S., Esposito, F., Tedeschi, G., 2013. Motor and extramotor neurodegeneration in amyotrophic lateral sclerosis: a 3T high angular resolution diffusion imaging (HARDI) study. Amyotrophic Lateral Sclerosis and Frontotemporal Degeneration 14, 553–561.
Turner, M.R., Agosta, F., Bede, P., Govind, V., Lulé, D., Verstraete, E., 2012. Neuroimaging in amyotrophic lateral sclerosis. Biomarkers Med. 6, 319–337.
Turner, M.R., Verstraete, E., 2015. What does imaging reveal about the pathology of amyotrophic lateral sclerosis? Current Neurol. Neurosci. Rep. 15, 45.
Tustison, N.J., Avants, B.B., Cook, P.A., Zheng, Y., Egan, A., Yushkevich, P.A., Gee, J.C., 2010. N4ITK: improved N3 bias correction. IEEE Trans. Med. Imaging 29, 1310–1320.
van der Knaap, L.J., van der Ham, I.J., 2011. How does the corpus callosum mediate interhemispheric transfer? A review. Behav. Brain Res. 223, 211–221.
Veraart, J., Fieremans, E., Novikov, D.S., 2016. Diffusion MRI noise mapping using random matrix theory. Magn. Reson. Med. 76, 1582–1593.
Wahl, M., Lauterbach-Soon, B., Hattingen, E., Jung, P., Singer, O., Volz, S., Klein, J.C., Steinmetz, H., Ziemann, U., 2007. Human motor corpus callosum: topography, somatotopy, and link between microstructure and function. J. Neurosci. 27, 12132–12138.
Wakana, S., Caprihan, A., Panzenboeck, M.M., Fallon, J.H., Perry, M., Gollub, R.L., Hua, K., Zhang, J., Jiang, H., Dubey, P., 2007. Reproducibility of quantitative tractography methods applied to cerebral white matter. NeuroImage 36, 630–644.
Welniarz, Q., Dusart, I., Roze, E., 2017. The corticospinal tract: Evolution, development, and human disorders. Dev. Neurobiol. 77, 810–829.
Wittstock, M., Meister, S., Walter, U., Benecke, R., Wolters, A., 2011. Mirror movements in amyotrophic lateral sclerosis. Amyotrophic Lateral Sclerosis 12, 393–397.
Zhang, J., Ji, B., Hu, J., Zhou, C., Li, L., Li, Z., Huang, X., Hu, X., 2017. Aberrant interhemispheric homotopic functional and structural connectivity in amyotrophic lateral sclerosis. J. Neurol. Neurosurg. Psychiatry 88, 369–370.